Supporting Information

Graphite Paper Anode with Low Lattice Mismatch Enables Corrosion Inhibited Zinc Batteries

Supplementary Fig. S1-11

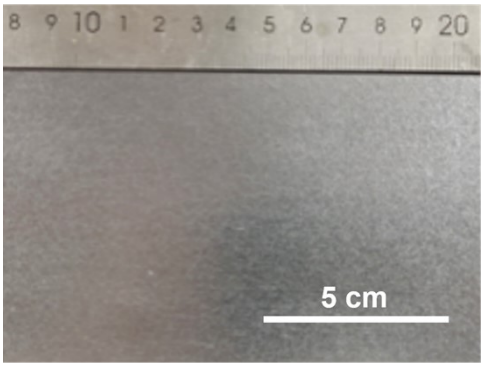

Fig. S1 Optical image of GP.

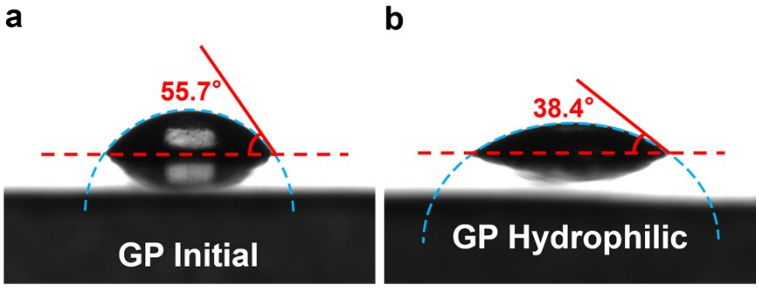

Fig. S2 Water contact angle of GP. (a) initial and (b)after vacuum plasma cleaning.

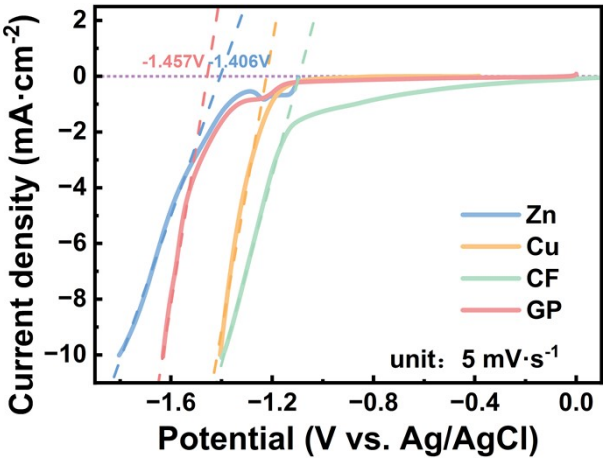

Fig. S3 LSV test of different materials in 7 M $CaCl_2$ solution with a scan rate of 5 $mV \cdot s^{-1}$.

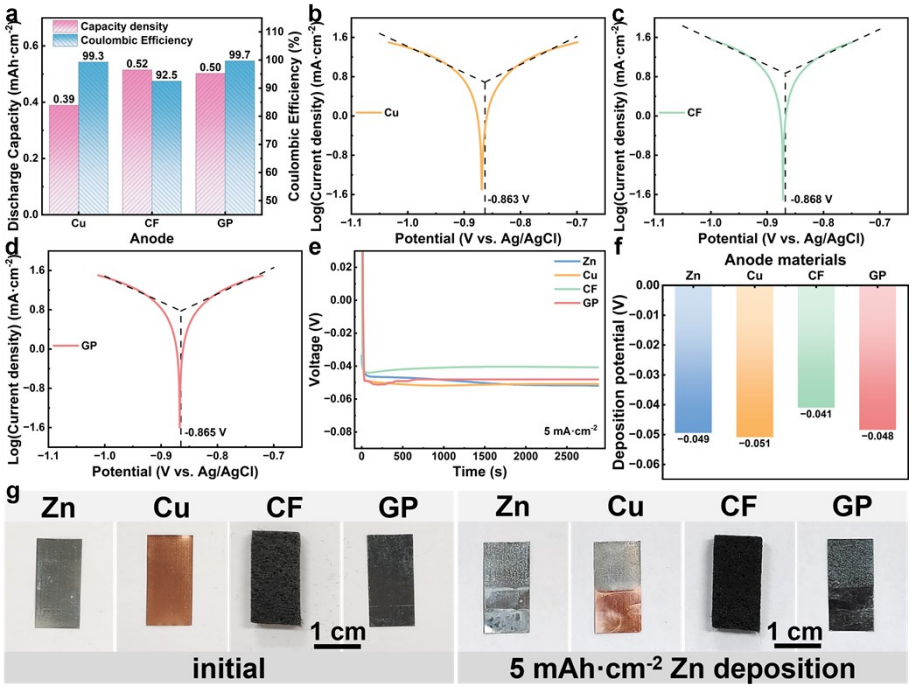

Fig. S4 (a) Discharge capacity curves and Coulombic efficiency curves of Cu, CF, and GP anodes in a single CV cycle. Tafel curves and fitted corrosion potentials of (b) Cu, (c) CF and (d) GP anodes. (e) Current-time curves and (f) Average deposition overpotentials of different materials during deposition at 5 mA·cm^{-2}. (g) Macroscopic optical images of different materials after depositing 5 mAh·cm^{-2} of Zn.

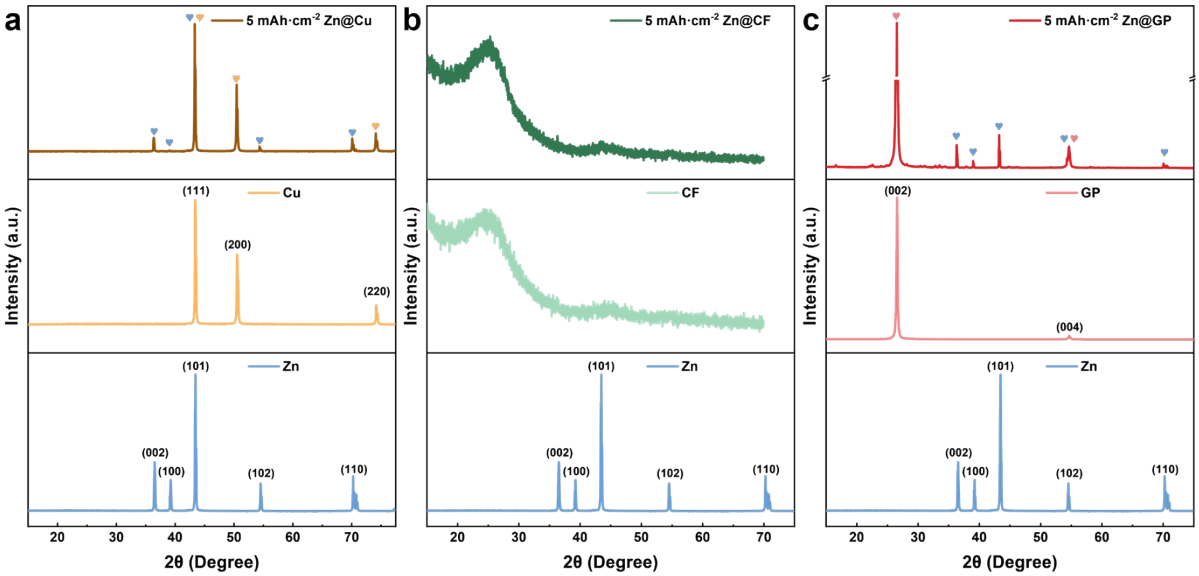

Fig. S5 (a-c) XRD patterns of Cu, GP, CF, as well as Zn@Cu, Zn@CF, and Zn@GP loaded with 5 mAh·cm^{-2} of Zn.

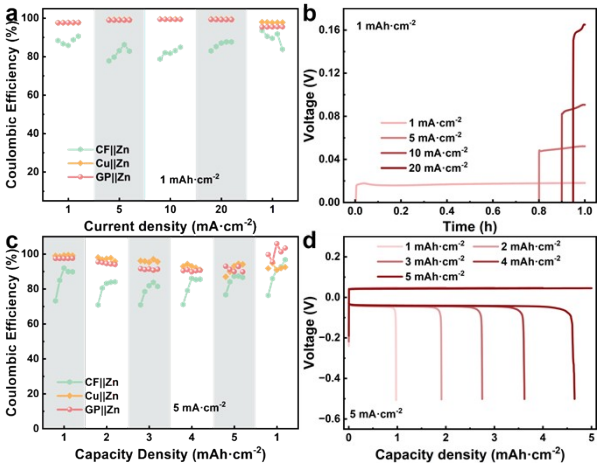

Fig. S6 (a) Current rate performance of GP||Zn, Cu||Zn, CF||Zn half-cells. (b) Deposition potential curves of GP|| Zn half-cell during current rate performance test. (c) Capacity rate performance of GP||Zn, Cu||Zn, CF||Zn half-cells. (d) Voltage-capacity curves of GP||Zn half-cell during capacity rate performance test.

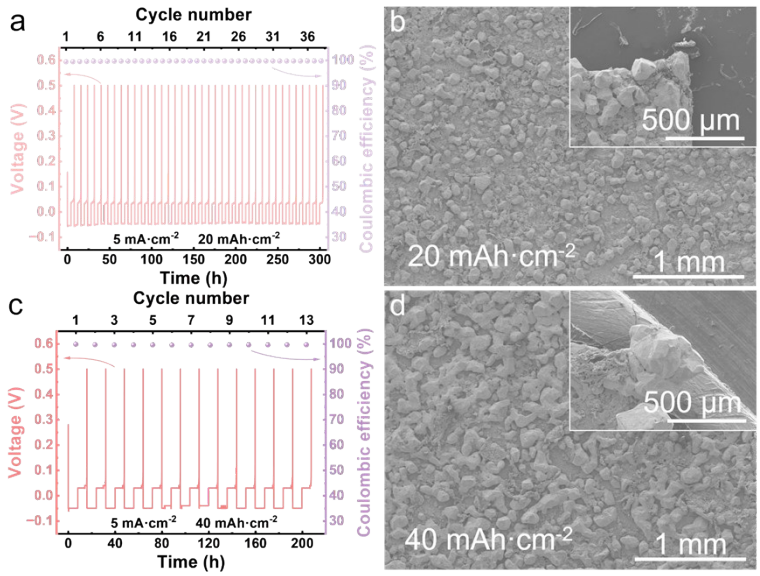

Fig. S7 (a) Deposition/dissolution performance and (b) SEM image at an areal capacity density of 20 mAh·cm^{-2}; (c) Deposition/dissolution performance and (d) SEM image at an areal capacity density of 40 mAh·cm^{-2}.

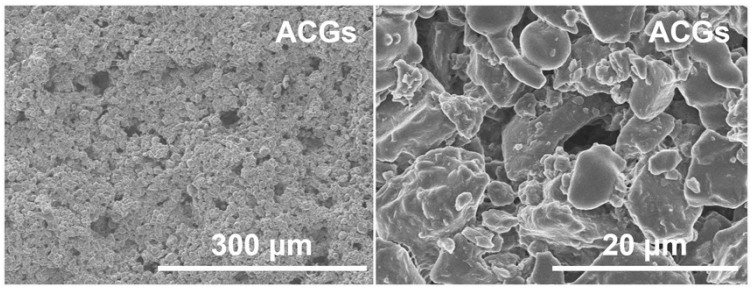

Fig. S8 SEM images of ACGs cathode at different magnification.

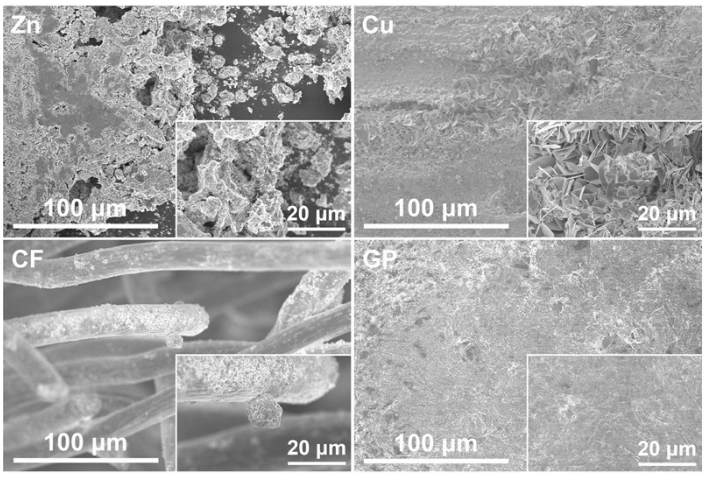

Fig. S9 SEM images of deposition/dissolution-type Zn-I_2 full cells with Cu, Zn, CF, and GP as anode after 150 cycles.

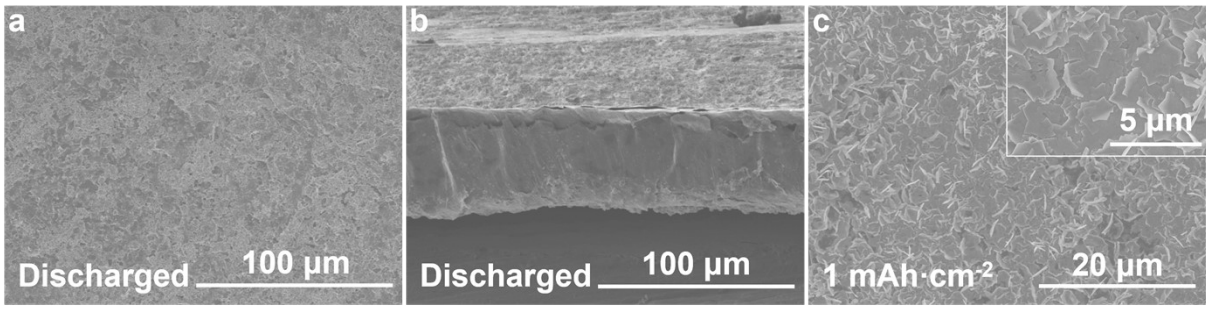

Fig. S10 (a) Surface and (b) cross-sectional SEM images of the full cell based GP anode after 500 cycles in a fully discharged state; (c) surface SEM image of the full cell after being charged to 1 mAh·cm^{-2}.

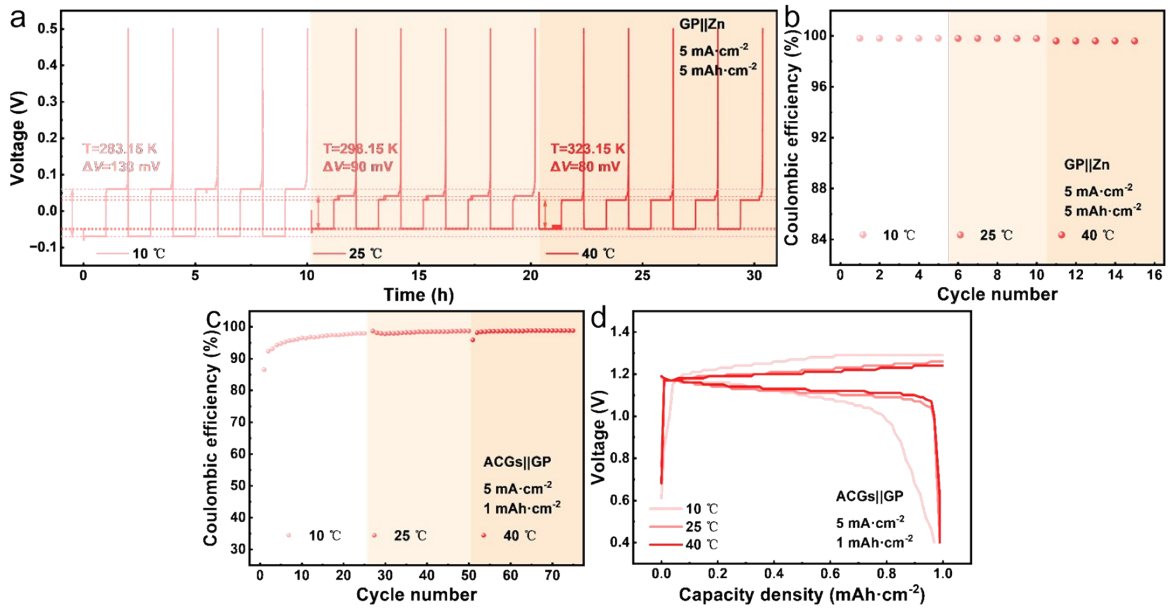

Fig. S11 (a-b)Half-cell deposition/dissolution performance and (c-d)full-cell cycling performance at different temperatures.

Supplementary Table S1-3

Table. S1 Electrical conductivity , density and specific surface areas of different materials.

Anode Materials	**σ(S·m^{-1})**	**ρ(g·cm^{-3})**	**specific surface areas(m^2·g^{-1})**
Cu	5.96×10^7	8.96	18.6×10^{-3}
Zn	1.69×10^{7z}	7.14	5.6×10^{-3}
GP	1.23×10^5	1.46	27.4×10^{-3}
CF	5.04×10^2	0.184	7 [1]

Table. S2 Capacity density and cycle lifespan of full cells under different strategies.

Strategy	Capacity density	Lifetime	Refs.
GP anode, ACGs cathode	**1 mAh·cm^{-2}**	**10000 (99.16% avg. CE)**	**This work (Zn-I$_2$)**
	3 mAh·cm^{-2}	**2500 (98.22% avg. CE)**	
silk protein additive	1.576 mAh·cm^{-2}	6000 (91.1% retained)	Zn-I$_2$ [2]
MXene cathode, n-butanol electrolyte additive, in-situ SEI protection	0.30 mAh·cm^{-2}	30000 (88% retained)	Zn-I$_2$ [3]
backside coated Zn foil	1.7 mAh·cm^{-2}	2000 (58.1% retained)	Zn-NVO [4]
self-assembled supramolecular bilayer	3.2 mAh·cm^{-2}	500 (64.7% retained)	Zn-Mn [5]

Table. S3 Cost and cycle life of the different electrode materials used in this study.

Materials	Thickness (μm)	Price (USD·m^{-2})	Cycle lifetime
GP	50	1.79	10,000
Zn foil	50	23.81	521
Cu foil	12	1.85	1,036

References

1 M. Schnucklake, L. Ka Ner, M. Mehring and C. Roth, *RSC Adv.*, 2020, **10**, 41926-41935.

2 S.J. Zhang, J. Hao, H. Wu, Q. Chen, C. Ye and S.Z. Qiao, *Adv. Mater.*, 2024, **36**, 2404011.

3 W. Yan, Y. Liu, J. Qiu, F. Tan, J. Liang, X. Cai, C. Dai, J. Zhao and Z. Lin, *Nat. Commun.*, 2024, **15**, 9702.

4 N. Yang, Y. Gao, F. Bu, Q. Cao, J. Yang, J. Cui, Y. Wang, J. Chen, X. Liu and C. Guan, *Adv. Mater.*, 2024, **36**, 2312934.

5 S. Chen, Y. Xia, R. Zeng, Z. Luo, X. Wu, X. Hu, J. Lu, E. Gazit, H. Pan, Z. Hong, M. Yan, K. Tao and Y. Jiang, *Sci. Adv.*, 2024, **10**, n2265.